

Molecular Simulation



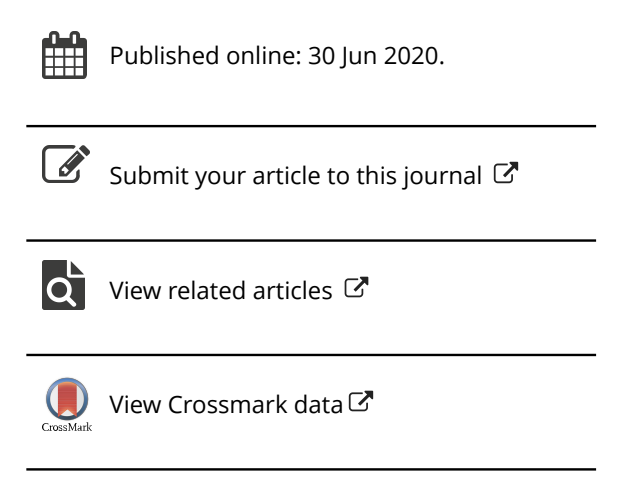
ISSN: (Print) (Online) Journal homepage: https://www.tandfonline.com/loi/gmos20

A review of recent advances in computational and experimental analysis of first adsorbed water layer on solid substrate

Guobing Zhou & Liangliang Huang

To cite this article: Guobing Zhou & Liangliang Huang (2020): A review of recent advances in computational and experimental analysis of first adsorbed water layer on solid substrate, Molecular Simulation, DOI: 10.1080/08927022.2020.1786086

To link to this article: https://doi.org/10.1080/08927022.2020.1786086







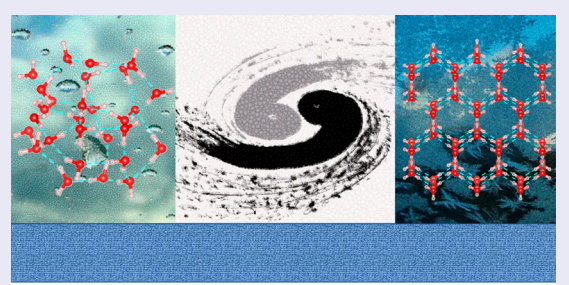
A review of recent advances in computational and experimental analysis of first adsorbed water layer on solid substrate

Guobing Zhou* and Liangliang Huang

School of Chemical, Biological and Materials Engineering, University of Oklahoma, Norman, OK, USA

ABSTRACT

The interactions at the water/solid interface is of great importance to a broad range of scientific phenomena and technological processes in astrophysics, electrochemistry, corrosion, lubrication, and heterogeneous catalysis. Tremendous research interest has been dedicated to comprehending the behaviours of water molecules near solid surfaces, particularly the first adsorbed water layer (FAWL) due to its dominant role in dictating mass and charge transport and influencing reaction rate and mechanism at the interface. In this review, we summarise the recent advances in the molecular-level understanding of the FAWL on solid substrates. We start by describing the evolution of the ice-like bilayer structures of FAWL on Ru(0001) and Pt(111) surfaces, followed by a brief discussion of substrate surface morphology effect on water structures. Subsequently, we discuss the molecular and dissociative adsorption structures of FAWL on metal oxide surfaces. After that, we interpret how the properties of FAWL affect the behaviour of water molecules above the monolayer. The summary and outlook towards the design and manipulation of ordered monolayer water is presented in the end.



First Adsorbed Water Layer at Solid Substrates

ARTICLE HISTORY

Received 6 April 2020 Accepted 12 June 2020

KEYWORDS

Water/solid interface; computation and experiment; first adsorbed water layer; adsorption structure

1. Introduction

Water is one of the most ubiquitous and important liquids on earth, and it involves a wide range of applications in biological, chemical, geological, and industrial processes. Compared to other fluids, water is a relatively simple substance consisted of one oxygen and two hydrogen atoms, which can separately act as acceptors and donors to form hydrogen bonds (HBs) with neighboring water molecules. Despite extensive studies over the past decades, investigating the nature of HB interaction and network is still far from complete. In particular, the behaviour of water at solid surfaces is of critical importance to numerous scientific and technological fields, including photocatalytic water splitting, heterogeneous catalysis, electrochemistry, materials science, and corrosion [1-7]. When liquid water approaches the solid surface, the HB network of bulk water will gradually change. Eventually, the adsorption structure of water at the interface will be governed by a subtle balance between water-solid and

water-water HB interactions. Such a dynamic balance determines the stability and other properties of FAWL at solid surfaces. To better understand the water/solid interface, the first critical step is to confirm where and how water molecules bind to the surface. This is challenging for experiments owing to the difficulty in detecting the binding motifs on specific surface sites and obtaining the details of structures and dynamics for the monolayer water sample on the solid substrate [7]. Consequently, a large number of experimental and theoretical studies have been reported with molecular-level insights into the chemical and physical properties of interfacial water using the state-of-art surface science techniques and calculation methods [1–3, 8–10].

For water molecules on the solid substrate, the adsorption structures are largely dependent on the intrinsic nature of the solid surface. When water molecules are deposited on an inert surface, both molecular and dissociative adsorption structures are possible [1–3, 8]. Moreover, the adsorption properties of interfacial water molecules are also significantly influenced

by the coverage since a higher coverage of water molecules on the surface can form extended HB networks [3]. In this context, a series of experimental characterisation techniques, including scanning tunnelling microscope (STM) [11-20], atomic tunnelling microscope (AFM) [21, 22], X-ray photoelectron spectroscopy (XPS) [11, 23-25], X-ray absorption spectroscopy (XAS) [11, 24], reflection-absorption infrared spectroscopy (RAIRS) [26], sum-frequency generation (SFG) spectroscopy [27], Low-energy electron diffraction (LEED) [28-35], and He atom scattering (HAS) [35, 36], have been extensively employed to probe the interfacial structures and properties of water on solid substrates. Wherein, STM and AFM are capable of providing atomistic-level resolution of real space images and HB network information for water clusters on distinct surfaces, which tremendously improves our understandings of the behaviours of interfacial water [7]. However, it is worth noting that STM images may be perturbed by the tip tunnel current since prior studies have demonstrated that the tip interactions can restructure or dissociate water molecules on the surface [37, 38]. When it comes to the identification of the species on the surface, XPS and XAS can determine whether the interfacial water is intact or partially dissociated, through characteristic spectroscopic peaks to identify OH groups from water dissociation, the first molecular layer of water, and other water. Meanwhile, XPS can provide a quantitative measurement of the dissociation degree of water film on solid surfaces [23]. On the other hand, XAS can detect the orientation of free OH groups at the interface [39]. Besides, IR spectroscopy also provides information of the HB network and the bonding environment of the water clusters on the surface. However, IR generally fails to assign specific adsorption structures. This is mainly due to the fact that despite vibrational frequency is an indicator to the HB strength, additional information is needed to reveal the local structure within the water cluster [3]. Overall, aforementioned characterisations provide insights into the interface and structural details of water at the surface. Yet, limitations exist if one only uses experimental techniques to understand the fundamental of interfacial water. For example, most experiments focus on the first adsorbed water layer (FAWL) at solid surfaces, little is known regarding the change of interfacial water properties when the thickness of water film changes. Alternatively, theoretical calculations and simulations can provide not only atomic details but also dynamic properties of the FAWL, as well as how the FAWL affects adsorption, nucleation, and reaction of other water at the interface.

Up to now, multiscale computational methods, including ab initio density functional theory (DFT), ab initio molecular dynamics (AIMD), reactive molecular dynamics (RxMD), and classical molecular dynamics (CMD), have been widely employed to study the liquid/solid interface, with an electronic and atomistic level details on structures and dynamics of interfacial water at various metal and metal oxide surfaces. As the basic building unit, the small water clusters determine the epitaxial growth of FAWL across the solid surface, and influence the packing of water film in the longitudinal direction [40]. Therefore, great efforts from ab initio DFT calculations have been dedicated to understanding the structures of water clusters on solid surfaces. Basically, DFT calculations are capable

of reproducing the adsorption sites, simulating the STM images, and predicting the dissociation and diffusion barriers of water molecules at the interface. However, it is worthwhile to mention that DFT calculation results are largely influenced by exchange-correlation (XC) functionals [41, 42] and van der Waals (vdW) corrections [43-46]. For example, Gillan and coworkers [41] discussed the employment of different functional methods, including the local density approximation (LDA), generalised gradient approximations (GGAs), and hybrids, to calculate the binding energy in H₂O dimer. They concluded that, compared to the benchmark value of 217.6 meV from CCSD(T) calculations, the LDA functional (380 meV) significantly overestimates the binding energy of the dimer by nearly a factor of 2. Similar overestimations have also been observed for PBEsol functional (2650 meV). On the contrary, functionals such as BLYP and revPBE underestimate the binding energy by 181 and 156 meV, respectively. So far, the best functionals to describe the binding energy in H₂O dimer are reported to be PBE (220 meV) and its hybrid version PBE0 (215 meV). Aside from the choice of XC functionals, it is also critical to include the correction to dispersion forces in DFT calculations. Most XC functionals fail to describe the non-local vdW dispersion forces. Recent dispersion-corrected DFT studies have indicated that the consideration of vdW dispersion forces can provide a more accurate description of interactions between water and solid substrates, as well as interactions between water layers on the surface [44-46]. It is recommended to benchmark the XC functionals and vdW corrections for the study of water behaviour at solid surfaces.

Although the DFT-based simulation method is a powerful tool to explore the properties of interfacial water, the computational cost inherent to the electronic-level calculations severely restricts us to explore the dynamic processes occurred at the interface for larger systems with extensive trajectory timescales. One alternative way to address this issue is to develop force field parameters by employing results from DFT calculations [47]. Empirical simulation methods that are based on those developed force fields, including RxMD and CMD, require remarkably fewer computational resources and enable the explore of a complex system up to micrometer and microsecond scales. For RxMD and CMD simulations, the big difference is that the RxMD is able to describe chemical reactions through a bond order concept [48], which is based on the interatomic distance. In particular, the transferability of the reactive force field (ReaxFF) for each element promotes RxMD simulations to model the complex interfacial processes between solid and liquid [48]. To date, ReaxFF parameter sets have been developed for more than 40 elements of the periodic table and have been successfully applied to numerous liquid/solid interface systems, including H₂O/TiO₂ [49, 50], H₂O/ZnO [51], H₂O/SiO₂ [52], H₂O/Si [53], H₂O/Ni [54], and H₂O/Cu [55], to just name a few. Yet we point out that development of ReaxFF is nontrivial, due to the large number of parameters implemented in the concept and formulations of ReaxFF. Meanwhile, it is noteworthy that reactive force fields aim at specific systems, and thereby the corresponding parameters can be quite different in spite of the same element in different systems. For example, in prior studies by van Duin and coworkers [50, 56], they developed two sets of reactive force

field for titanium dioxide (TiO2): one is to describe the interactions between TiO₂ and H₂O, and the other one is to simulate the etching of TiO₂ with Cl₂ and HCl gases. There is a significant difference in the force field parameters of Ti element. Therefore, we should pay a special attention to the choice of reactive force fields when performing the RxMD simulations. For non-reacting systems of water on solid surfaces, CMD simulations provide equivalent accuracy of predictions and similar level of insights of diffusion, wetting, and ice nucleation. of water on solid surfaces. For the CMD simulations, the choice of the force field is an important factor to the accuracy of simulation results. In prior studies, numerous functional forms with distinct force fields have been proposed to describe the interactions between water molecules and solid surfaces, including Morse [57], Buckingham [57, 58], GAL19 [59], and Lennard-Jones (L-J) (12-6, 10-4, 9-6, and 9-3) [57, 60, 61] potentials. Among all reported potentials, the L-I potentials are the most widely adopted parameters to simulate the liquid-solid interface, but occasionally the Morse and Buckingham potentials might provide a better description. For example, the study by Johnston and coworkers [57] demonstrated that the L-J potential did not reproduce the DFT water-gold configurational energy landscape, whereas the softer Morse and Buckingham potentials allowed for a more accurate representation. On the other hand, the water model is another critical factor for CMD simulations and different models show distinct performance in reproducing the water properties. Wherein, the SPC/E and TIP4P/2005 models are capable of providing a better prediction in surface tension compared to the TIP3P, TIP4P, and TIP5P models [62]. Moreover, they also show a great performance in predicting the self-diffusion coefficient [62], which is in an excellent agreement with experiments. In addition, TIP4P/ 2005 is also able to simulate the entire phase diagram of condensed water [63], while TIP4P/Ice is useful for the investigation of both ice Ih and denser ice form [64].

In this review, we briefly summarise the recent progress in experimental and theoretical understanding of the FAWL at solid substrates, with the special attention to how the formation and behaviour of FAWL influence structural and chemical properties of the surface. In Section 2, we elaborate the adsorption structures of FAWL on metal surfaces, followed by an overview on the FAWL on distinct metal oxide surfaces in Section 3. Section 4 presents the discussions of how the properties of FAWL affect the behaviours of other water molecules above the monolayer. Finally, we conclude in Section 5 with the summary and outlook towards the design and manipulation of the FAWL.

2. The FAWL on metal surfaces

When water molecules are in contact with metal surfaces, their adsorption structures are determined by combined contributions of water-metal and water-water interactions. For an isolated water molecule on metal surface, the binding energy is in the range of 0.1–0.5 eV [65], comparable to that of a water in bulk ice, and the OH groups prefer the orientation parallel to the surface. With the increase of water coverage, there would form an intact water overlayer with $(\sqrt{3} \times \sqrt{3})R30^{\circ}$ structure on a few close-packed transition metal surfaces [1,

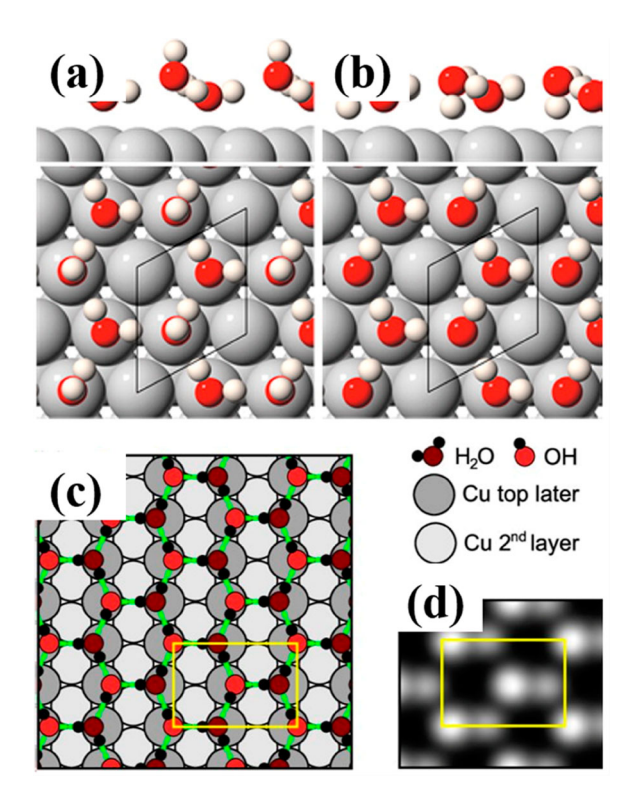


Figure 1. (Colour online) Schematic illustration for an ordered $(\sqrt{3} \times \sqrt{3})R30^{\circ}$ water structure with (a) H-up and (b) H-down configurations on a close packed surface. (c) optimised structures and (d) simulated STM images for the stoichiometric $c(2 \times 2)$ overlayer on Cu(110) surface. (a,b) Reproduced with permission from Ref. [1]. Copyright (2016) American Chemical Society. (c,d) Reproduced with permission from Ref. [67]. Copyright (2011) American Physical Society.

3, 7]. Later, an 'ice-like' bilayer structure was proposed to interpret the $(\sqrt{3} \times \sqrt{3})R30^{\circ}$ structure, considering a close match between their lattice parameter and the lattice spacing in ice Ih(0001) [3, 7, 66]. As illustrated in Figure 1(a), the bilayer model has a buckled hexagonal network. Wherein, the lower water molecules directly interact with surface metal atoms via their oxygen atoms, while the upper molecules are stabilised through the HB interactions with neighboring water molecules. In addition, on the face-centered-cubic (FCC) (110) surface, a $c(2 \times 2)$ structure was observed for the FAWL, which has distorted hexagonal network to fit the rectangular unit cell [3, 67]. Indeed, the adsorption structures of water on metal surfaces are very complicated because of their sensitivity to both chemical nature and geometry of solid substrates. Therefore, a better understanding of water structures on distinct metal surfaces relies on the cooperation of experimental measurements and theoretical calculations.

2.1. Water on Ru(0001) surface

The pioneering investigation on water adsorption on metal surface is $H_2O/Ru(0001)$, due to its smallest lattice mismatch with bulk ice compared to other transition metal surfaces [3, 5]. Previous LEED studies reported that the wetting layer on Ru(0001) adopts an 'ice-like' bilayer structure with a $(\sqrt{3} \times \sqrt{3})R30^{\circ}$ phase [28]. Later, Held and Menzel [29] presented the first complete intensity-voltage LEED analysis of an ordered water bilayer structure adsorbed on Ru(0001) surface. In their

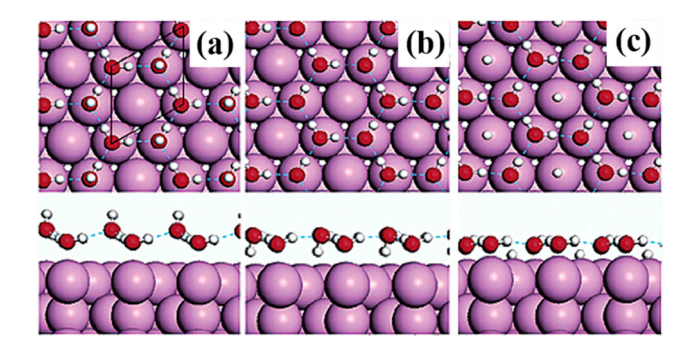


Figure 2. (Colour online) Top and side views of (a) 'H-up' intact bilayer, (b) 'Hdown' intact bilayer, and (c) the partially dissociated OH-H₂O + H overlayer on Ru(0001) surface. Reproduced with permission from Ref. [68]. Copyright (2003) American Chemical Society.

observed $(\sqrt{3} \times \sqrt{3})R30^{\circ}$ structure, the vertical distance between the O atoms in the bilayer was found to be only 0.10 Å, rather than the 0.96 Å as observed in ice I_h . Besides, the DFT calculations by Feibelman [30] showed that the adsorption energy of intact water layers with coplanar O atoms lie 0.15-0.20 eV below the heat of sublimation of ice-Ih. Alternatively, The energetics and adsorption geometries of half-dissociated structures are in much better agreement with experiment. Analogously, King and coworkers [68] found that a partially dissociated OH + H₂O overlayer (see Figure 2 (c)) is energetically favoured over pure intact H₂O bilayers (Figure 2(a,b)) on the surface. Also, they further reported that the barrier of a chemisorbed H₂O monomer dissociation is 0.8 eV, whereas the barrier to dissociate a H₂O in a bilayer is only 0.5 eV.

Since the discovery of mixed H₂O/OH in the wetting layer on Ru(0001) surface, great efforts from both experimental and theoretical studies have been devoted to the unique water overlayer [1, 3, 5, 7, 11, 12, 26, 68-71]. For example, Kim et al. [26] examined the acid-base properties of a water film adsorbed on the Ru(0001) surface, by means of RAIRS, low-energy sputtering, temperature-programmed desorption, and reactive ion scattering. They found that only the water molecules in an intact water monolayer or water clusters larger than the hexamer exhibit the acidity. However, a thick ice film and a partially dissociated water monolayer that contains OH, H₂O and H species are not acidic. Tatarkhanov et al. [11] investigated the water structures on Ru (0001) surface through a combination of STM, XAS, and DFT calculations. They found a stable partially dissociated H₂O-OH phase of water adsorbed on Ru(0001) at 180 K, and the XPS and XAS results revealed an average ratio of 3:1 for H₂O and OH. Furthermore, the STM measurements and DFT calculations results showed that the mixed H₂O-OH phase has a honeycomb structure forming elongated stripes, with H₂O molecules preferentially lay flat and OH groups to be inside the stripes [11]. Salmeron and coworkers [12] used the STM to probe the structure and growth of the first few layers of water on Ru(0001) at 140 K, and their results demonstrated that the molecular structure of FAWL consists of hexagonal water rings with two orientations. One is in registry with the hexagonal metal surface and covalently bonded through the oxygen atoms. The other one is rotated by 30° and slightly lifted off the substrate. These two orientations are connected by pentagonal and heptagonal rings. In addition, Messaoudi et al. [69] explored the wetting of intact and partially dissociated water layers on Ru(0001) surface via DFT calculations. They found that, for the first bilayer on Ru(0001) surface, a partial dissociation of 3/8 of the water molecules (Figure 3(b)) is slightly more stable than the half-dissociation (Figure 3(c)). Moreover, such kind of bilayer structure contains H-up water molecules pointing to the vacuum. This makes the wetting of the first water layer on Ru(0001) more favourable for the partially dissociated structure compared to the intact one.

2.2. Water on Pt(111) surface

An early LEED study by Firment and Somorjai [31] demonstrated that the wetting layer on Pt(111) surface has a simple commensurate $(\sqrt{3} \times \sqrt{3})R30^{\circ}$ structure. However, later STM studies reported that the bilayer structure resulting from the exposure of Pt(111) to H₂O at 140 K has four different phases, only part of which exhibits the $(\sqrt{3} \times \sqrt{3})R30^{\circ}$ structure [13]. Also, the HAS [36] and LEED [32, 33] further revealed that the water overlayer on Pt(111) surface forms two highly ordered and epitaxially rotated water phase, namely $(\sqrt{37} \times \sqrt{37})R25.3^{\circ}$ and

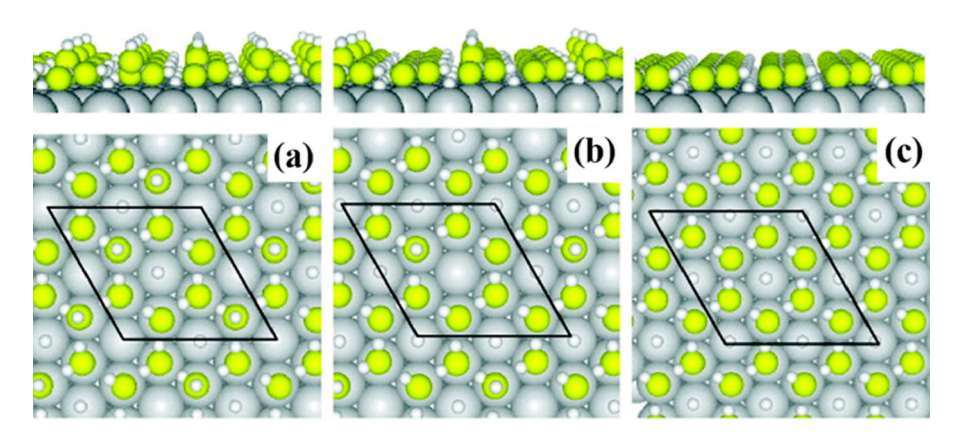


Figure 3. (Colour online) Top and side views of mixed water overlayer on Ru(0001) surface with a OH/H₂O ratio of (a) 1/4, (b) 3/8, and (c) 1/2. Reproduced with permission from Ref. [69]. Copyright (2011) American Chemical Society

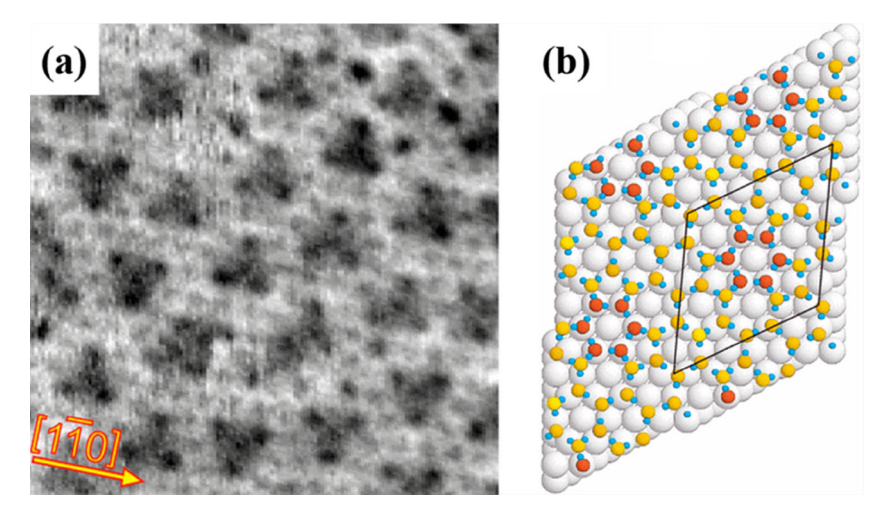


Figure 4. (Colour online) (a) STM image and (b) √37 phase structure of monolayer water on Pt(111) surface. Reproduced with permission from Ref. [14]. Copyright (2010) American Physical Society.

 $(\sqrt{39} \times \sqrt{39})R16.1^{\circ}$. These two phases show slightly difference in their density and alignment with respect to the surface. Meanwhile, it is reported that the $(\sqrt{37} \times \sqrt{37})R25.3^{\circ}$ structure first forms at submonolayer coverage, and it then compresses to form the $(\sqrt{39} \times \sqrt{39})R16.1^{\circ}$ structure when the coverage is at saturation [33]. To gain more details on the water overlayer on Pt(111) surface, Ogasawara et al. [24] used XAS and XPS to separately probe the orientation of free OH groups in the water molecules and the bonding of water to Pt surface. Their results showed that all water molecules in the FAWL bind directly to the surface via alternating metal-oxygen (M-O) and metal-hydrogen (M-HO) bonds, forming a nearly flat overlayer with the H-down configuration.

In response to the experimental results, a number of theoretical studies have been performed to examine the water structures on Pt(111) surface [14, 15, 72–75]. By means of ab initio molecular dynamics simulation, Meng et al. [72] investigated the adsorption structures and vibrational spectra of H-up and H-down $(\sqrt{3} \times \sqrt{3})R30^{\circ}$ bilayer. Their calculation results showed that the vibrational frequencies for the bilayer, either H-up or H-down case, agree well with the experimental data. However, the adsorption energy results revealed that the Hdown structure (534 meV) is slightly more stable compared to the H-up one (522 meV) [73], which is in good agreement with the DFT results by Michaelides and coworkers [74]. Besides, Meng et al. [73] also determined the adsorption structures for the water overlayers on Pt(111) surface with $(\sqrt{37} \times \sqrt{37})R25.3^{\circ}$ and $(\sqrt{39} \times \sqrt{39})R16.1^{\circ}$ phases. They obtained an adsorption energy of 597 meV for the former and 615 meV for the latter, compared to a corresponding value of 534 meV for the $(\sqrt{3} \times \sqrt{3})R30^{\circ}$ phase. Such results confirmed that the $(\sqrt{37} \times \sqrt{37})R25.3^{\circ}$ $(\sqrt{39} \times \sqrt{39})R16.1^{\circ}$ structures are more stable than the $(\sqrt{3} \times \sqrt{3})R30^{\circ}$ structure. Also, Meng [75] found that the $(\sqrt{39} \times \sqrt{39})R16.1^{\circ}$ bilayer structure shows a quite disordered arrangement, with the O atoms lying in three different heights between 2.2 and 4.5 Å above the Pt surface. This is opposite to the flat bilayer model proposed by Ogasawara et al., who found that the vertical thickness between the upper and lower O

atoms is only up to 0.25 Å [24]. Moreover, the ab initio MD simulations by Meng [75] revealed $(\sqrt{39} \times \sqrt{39})R16.1^{\circ}$ bilayer structure consists of 20% water molecules in the first flat layer and 66% in the second layer, as well as a small fraction of dissociated water molecules. Such dissociation is ascribed to both lateral compression of the water film and its interaction with the Pt substrate. An improved understanding of the water arrangement on Pt (111) surface is realised by the high resolution STM images [14-17], which uncover dark triangular depressions embedded in a hexagonal rings of water molecules (Figure 4(a)). These molecules are rotated approximately 30° relative to the classic commensurate $(\sqrt{3} \times \sqrt{3})R30^{\circ}$ bilayer. The simulated STM images from DFT calculations reproduce the experimentallyobserved dark triangular features for $(\sqrt{37} \times \sqrt{37})R25.3^{\circ}$ and $(\sqrt{39} \times \sqrt{39})R16.1^{\circ}$ structures [14]. Wherein, the wetting layer is built from a hexamer (see the red O atoms in Figure 4(b)) lying flat on the surface with O atoms in atop sites. This hexamer unit is surrounded by fiveand seven-membered rings(see the yellow O atoms in Figure 4(b)) that embed within the hexagonal water network, as shown in Figure 4(b).

2.3. Water on stepped Pt surface

As we discussed above, the FAWL can be significantly influenced by the intrinsic nature of underlying metal substrates. Meanwhile, it is reported that the surface morphology, such as steps and terraces, also plays a key role in the structures of FAWL [18-20, 65, 76-79]. Till now, numerous studies have been carried out to probe the behaviour of water molecules on stepped metal surfaces, particularly for Pt surface [18-20, 76-83]. For example, Nakamura and coworkers [81] used the surface X-ray diffraction to explore the water structures on Pt(211) surface, which has (100) steps separated by 3 atom wide terraces (see the illustration in Figure 5(a)). They observed that the water molecules can form one-dimensional (1D) zigzag chain along the steps via HBs interactions. Such configuration is supported by the O K-edge X-ray absorption fine structure

Figure 5. (Colour online) Schematic illustration of top and side views of (a) Pt(211), (b) Pt(221), (c) Pt(533), and (d) Pt(553) surfaces.

spectroscopy [82]. A DFT study by Donadio and coworkers [83] demonstrated that water on Pt(221) (see the illustration in Figure 5(b)) surface also preferentially binds to the step edge to form linear clusters or chains. Moreover, they observed that the water molecules would undergo a partial dissociation to generate a mixed hydroxyl/water structure through an autocatalytic mechanism [78]. For comparison, the DFT calculation results by Pekoz and Donadio [77] revealed that there is a more weak adsorption for water molecules at the step edges of Pt (211) compared to Pt(221), but the partial dissociation of the adsorbed water molecules is energetically competitive. In addition, a combination of STM measurements and DFT calculation studies by Kolb et al. [20] reported that the water molecules can form double-stranded networks with tetragonal structures at the (111) step of Pt(553) (see the illustration in Figure 5(d)) surface. Meanwhile, they also determined the adsorption geometries and energetics of water on and near the step edge of the Pt(533) (see the illustration in Figure 5 (c)) surface, and found multiple water structures with similar energies when a full water coverage is considered [79]. More recently, Jiang and coworkers [76] studied the water structures on Pt(221) and Pt(553) surfaces by employing a genetic algorithm method on top of DFT. Their calculation results uncovered a number of novel 1D chain and two-dimensional (2D) network. Particularly, it is interesting to find that the step-in

substrate is beneficial for the formation of 1D water chain, while the terrace is important for the formation of 2D water networks.

When water molecules are deposited on Ru (0001) and Pt (111) surfaces, they form monolayer water structures on both surfaces. However, the configurations of the FAWL for the two surfaces are significantly different. For the Ru (0001) surface, the FAWL adopts an ice-like structure with a $(\sqrt{3} \times \sqrt{3})R30^{\circ}$ periodicity, as confirmed by both experimental measurements and theoretical calculations, see Table 1 [11, 28, 30, 68, 69]. Other studies also pointed out that water molecules of the FAWL would dissociate to produce OH + H species, and that the mixed OH/H2O wetting layer is much more energetically stable than the intact water overlayer [69]. When it comes to the Pt(111) surface, the $(\sqrt{3} \times \sqrt{3})R30^{\circ}$ structure was reported for the FAWL, which has a lateral expansion of 6% compared to the bulk ice bilayer [3, 13, 31]. However, recent studies reported that water molecules on Pt (111)surface would first form structure a $(\sqrt{37} \times \sqrt{37})R25.3^{\circ}$ and then transition $(\sqrt{39} \times \sqrt{39})R16.1^{\circ}$ structure, wherein the former has a slight expansion of 3.6% and the latter shows a compression of 4.4% [33]. Moreover, the results from DFT calculations demonstrated that the $(\sqrt{37} \times \sqrt{37})R25.3^{\circ}$ and $(\sqrt{39} \times \sqrt{39})R16.1^{\circ}$ structures are more stable than the $(\sqrt{3} \times \sqrt{3})R30^{\circ}$ structure

Table 1. A summary of the unit cell, adsorption state, characterisation method, vertical distance between the O atoms in the bilayer structure, and ratio of H₂O/OH for the FAWL on Ru(0001) and Pt(111) surfaces.

Surface	Unit cell	Adsorption state	Characterisation	Dz _{O-O} (Å)	Ratio of H ₂ O/OH	Reference
Ru(0001)	$(\sqrt{3}\times\sqrt{3})R30^{\circ}$	Molecular	LEED		1:0	[28]
	$(\sqrt{3}\times\sqrt{3})R30^{\circ}$	Dissociative	DFT	0.05-0.06	1:1	[30, 68]
	$(\sqrt{3}\times\sqrt{3})R30^{\circ}$	Dissociative	STM, XAS, DFT	0.2	3:1	[11]
	$(\sqrt{3}\times\sqrt{3})R30^{\circ}$	Dissociative	DFT		8:3	[69]
Pt(111)	$(\sqrt{3}\times\sqrt{3})R30^{\circ}$	Molecular	LEED, STM		1:0	[13, 31]
	$(\sqrt{37\times37})R25.3^{\circ}$	Molecular	HAS, LEED, STM		1:0	[14, 32, 33, 36]
	$(\sqrt{39}\times39)R16.1^{\circ}$	Molecular	HAS, LEED, STM		1:0	[14, 32, 33, 36]
	$(\sqrt{3}\times\sqrt{3})R30^{\circ}$	Molecular (H-up)	DFT	0.63	1.0	[72]
	$(\sqrt{3}\times\sqrt{3})R30^{\circ}$	Molecular (H-down)	DFT	0.35	1.0	[72]
	$(\sqrt{3}\times\sqrt{3})R30^{\circ}$	Dissociative	DFT	0.06	1:1	[72]
	$(\sqrt{37\times37})R25.3^{\circ}$	Molecular	DFT		1:0	[73]
	$(\sqrt{39}\times39)R16.1^{\circ}$	Molecular	DFT		1:0	[73]

[73]. Different from the planar metal surfaces, the stepped Pt surfaces have step and terrace sites, making the structures of FAWL different from those on Ru(0001) and Pt(111) surfaces. For example, water molecules can form respectively distinct structures of 1D chain and 2D networks on Pt(221) [76, 78, 83] and Pt(553) [20] surfaces, see Table 2. It is also worth noting that water molecules on diverse stepped Pt surfaces can show different adsorption states and configurations, which is closely related to the water coverage on the surface.

3. The FAWL on metal oxide surfaces

For the metal oxide surfaces, the water molecules can be adsorbed chemically or physically on distinct surface active sites, including unsaturated metal sites, acid or base sites, and defect sites. This makes the water structures on oxide surfaces more complicated than those on metal surfaces. Besides, compared to the weak adsorption on metal surfaces, water molecules generally have strong interactions with oxide surfaces. As a result of this, it may result in the water dissociation on the unsaturated metal or defect sites. Furthermore, it is reported that the adsorption and/or dissociation of water molecules on some oxide surfaces can lead to surface reconstruction [2], making it a great challenge to explore the water behaviours at the interface from experiments. In this regard, different water structures, like multiple rings, 1D chain, 2D network, and various ice forms, have been reported from both experiments and calculations [1, 2, 9, 84, 85]. During the past years, using the advanced surface science techniques, including STM and AFM, combined with theoretical calculations, provides us a direct image on local structures of interfacial water molecules, and thereby enables us to obtain numerous groundbreaking understandings in this aspect. Herein, we will discuss the recent studies related to the adsorption structures of water

Table 2. A summary of the surface model, adsorption state, configuration, and characterisation method for the FAWL on different stepped Pt surfaces.

	Adsorption			
Surface	state	Configuration	Characterisation	Reference
Pt(211)	Molecular	1D Chain	XRD	[81]
Pt(211)	Dissociative	1D Chain	DFT	[77]
Pt(221)	Dissociative	1D Chain or Cluster	DFT	[76, 78, 83]
Pt(553)	Molecular	Double-Stranded Chain	STM, DFT	[20]
Pt(533)	Molecular	Ring, 1D Chain	DFT	[79]

molecules on several widely studied oxide surfaces, with special attention being paid to the FAWL.

3.1. Water at TiO₂ surfaces

Understanding the behaviour of water molecules at titanium dioxide (TiO2) surfaces is of great significance to promote further progress in practical applications of TiO₂ [86–88]. In nature, TiO2 exists in three crystal forms: rutile, anatase, and brookite, among which the extensive studies mainly focus on the interaction of water with rutile and anatase. From the structural point of view, the topmost TiO₂ surface consists of under-coordinated titanium (Ti) and oxygen (O) sites. These sites can interact strongly with interfacial water molecules and affect significantly the adsorption structures of water molecules on TiO2 surfaces. In the past decades, great efforts have been made to investigate the H2O/TiO2 system, from ab initio quantum mechanics calculations to force-field-based molecular dynamics simulations [8, 49, 50, 89]. In the review by Sun et al. [8], they summarised the theoretical insights into the H₂O/TiO₂ interactions. Specifically, for the rutile (110) surface, an intact water structure is observed at a full monolayer coverage, whereas a mixed OH/H₂O structure is proposed at a low water coverage (e.g. 1/8 monolayer) because of a partial dissociation [90]. In the case of water molecules on rutile (100) surface, earlier experimental studies reported a molecular adsorption structure [91], while recent spectroscopy results showed that a dissociated adsorption is favourable [92]. Such discrepancies also exist among the theoretical studies, probably due to the different methods and functionals employed in the calculations [8]. When it comes to rutile (011) surface, the DFT calculations revealed that water molecules can dissociate to produce the Ti_{5c}-OH and O_{2c}-H species on this surface [93]. On the other hand, the combined experimental and theoretical work by Beck et al. [94] showed that rutile (011) surface exhibits a (2×1) reconstruction with onefold coordinated (titanyl) O atoms. Later, Diebold and coworkers [95] explored the water structures on the reconstructed rutile (011) surface. They found that a mixed molecular/dissociative layer is the most stable configuration at low temperatures, whereas a fully dissociative layer appears when the temperature increases to 250 K. As for anatase surfaces, the studies of Vittadini and coworkers [96, 97] reported that the molecular adsorption is favoured on the anatase (101) surface.

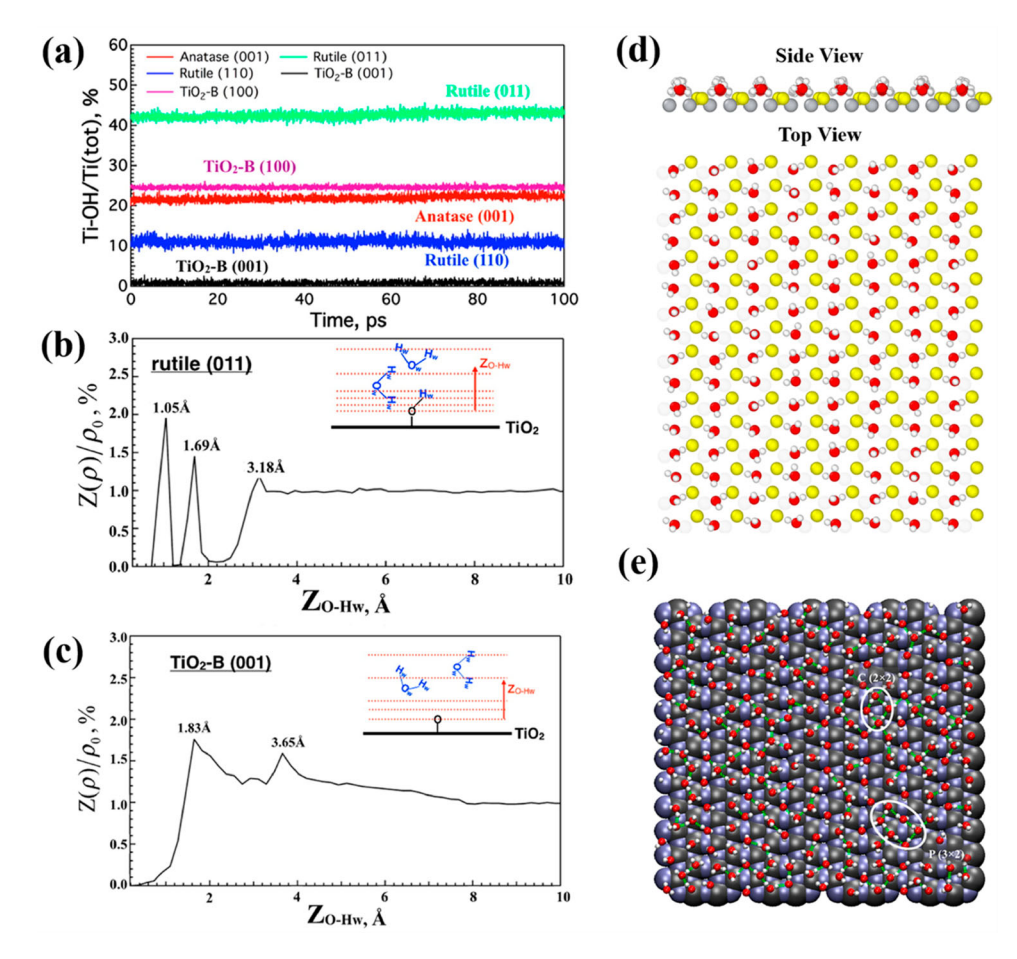


Figure 6. (Colour online) (a) Surface hydroxyl group density evolution: Ti-OH is the number of titanium atoms that are bonded with the OH groups from water dissociation, Ti(tot) is the total number of surface Ti atoms; density distribution of water molecules along the z direction: (b) rutile (011) with three distinct peaks and (c) TiO₂-B (001) with two distinct peaks; (c) structure of FAWL at rutile (011) interface, and (d) top view of the FAWL on the TiO₂-B (001) surface at t = 20.0 ns. HB-assisted water clusters. The HBs are in green, while the Ti and O atoms are coloured by gray and blue, respectively. (a-c) Reproduced with permission from Ref. [49]. Copyright (2014) American Chemical Society. (d, e) Reproduced with permission from Ref. [100]. Copyright (2018) American Chemical Society.

Meanwhile, it is found that the O atom in water molecule binds to the surface Ti_{5c} atom and two H atoms form HBs with the surface bridge O atoms. However, other calculation and XPS results proposed a mixture of dissociated and molecular water in the FAWL [25, 98, 99]. For anatase (001) and (100) surfaces, theoretical calculations showed that a low

coverage would lead to dissociative adsorption of water molecules on the surfaces, while a mixed molecular/dissociative adsorption was only observed for (001) surface at a full coverage [8].

Despite great progress in understanding of water behaviours on TiO₂ surfaces in the relatively low humidity, it is still unclear

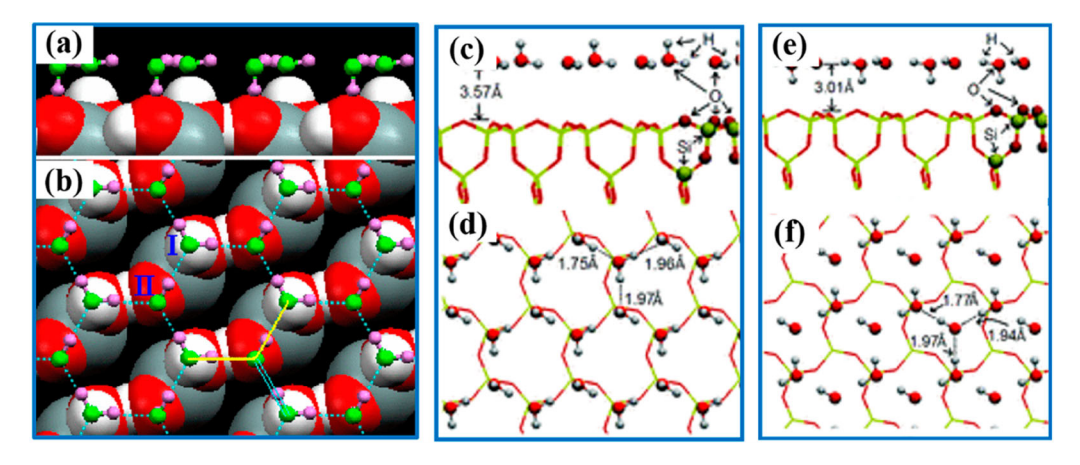


Figure 7. (Colour online) (a, b) Optimised H-down bilayer geometry on the hydroxylated α-quartz (0001) surface. Dotted lines denote the HB interactions between adsorbed molecules. Water monolayer adsorbed on α-quartz (0001) surface with (c, d) H-up and (e, f) H-down states. (a, b) Reproduced with permission from Ref. [102]. Copyright (2006) American Physical Society. (c-f) Reproduced with permission from Ref. [104]. Copyright (2011) American Physical Society.

on what happens if the TiO₂ surface is in contact with bulk water, and how water dissociation affects the behaviour of near-surface water on TiO₂ surfaces. To this end, we performed RxMD simulations to study the interactions between water and five different TiO2 surfaces. Our results showed that TiO2 surfaces demonstrate different reactivities for water dissociation [rutile (011) > TiO_2 -B (100) > anatase (001) > rutile (110)] (see Figure 6(a)), and there is no water dissociation observed on the TiO₂-B (001) surface [49]. Furthermore, it can be seen from Figure 6(b) that the new functional OH groups from the water dissociation in the FAWL on rutile (011) surface significantly enhance the interactions with near-surface water, and in turn it brings the second water layer closer to the surface. On the nonreactive TiO2-B (001) surface without any dissociative water adsorption, the near-surface water can form HB networks with the surface oxygen atoms of TiO2, but the distance of FAWL from the surface is larger than that from rutile (011) surface (see Figure 6(b,c)). On the other hand, our CMD simulations [100] showed that water molecules lean on rutile (011) surface with one H atom directing to the surface two-coordinated O atoms, and the other one pointing toward bulk water, as shown in Figure 6(d). For TiO2-B (001) surface, water molecules in the FAWL show a random distribution, yet, the in-layer HBs promote the formation of small water clusters near the surface (see Figure 6(e)).

3.2. Water at SiO₂ surfaces

Silica is widespread on the Earth's crust in amorphous or crystalline forms, i.e. quartz, cristobalite, trydimite [9, 85, 101]. Amongst these reported phases, the α-quartz is found to be the most stable one over a wide range of extreme conditions [9, 101], making it to be a typical model to explore the silicawater interactions in the natural and industrial processes. Yang and Wang [102], by combining the ab initio DFT calculations and AIMD simulations, investigated the water adsorption on hydroxylated α-quartz (0001) surface at various water coverages. For an isolated water monomer on the surface, it is found to be located above the bridge site between two surface hydroxyl groups and stabilised by forming two HBs with these two hydroxyl groups. Upon increasing the coverage to full monolayer, water molecules can form a flat ice-like bilayer structure with a puckered hexagonal network [102]. As shown in Figure 7(a,b), there are two types of water molecules

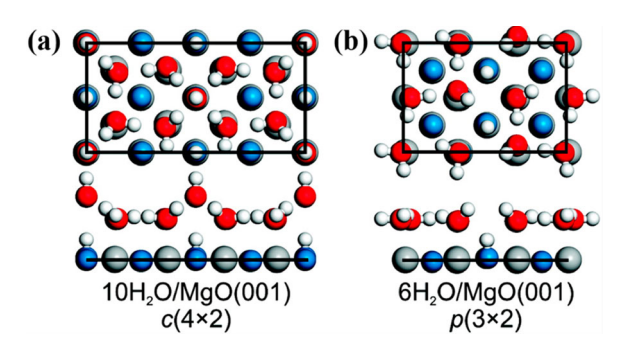


Figure 8. (Colour online) Side and top views of the most stable structures of (a) $10H_2O/c(4 \times 2)$ and (b) $6H_2O/p(3 \times 2)$. Reproduced with permission from Ref. [109]. Copyright (2011) American Chemical Society.

in this bilayer structure. Type I has the OH groups nearly parallel to the surface, whereas, in type II, each water molecule points one hydroxyl group to the surface to form the HBs. The vertical distance between these two types of water molecules is only 0.1Å, which is much smaller than the values observed for the bilayer structure in bulk ice (0.96Å) [103]. Such great compression primarily derives from the strong HB interactions within the monolayer water and with the surface hydroxyl groups. Chen and coworkers [104] studied the interactions between thin water films and α-quartz (0001) surfaces by using first-principles DFT calculations. They showed that the FAWL on the (1×1) bare surface has two distinct adsorption states: One has its out-of-plane hydrogen pointing up (H-up) (see Figure 7(c,d)) and the other one has its out-ofplane hydrogen pointing down (H-down), as shown in Figure 7 (e,f). For the H-up configuration, all water molecules in the FAWL prefer to be located above the surface silicon atoms. For the H-down configuration, only half of the water molecules in the FAWL reside the atop site, while the other half tends to be adsorbed on the surface hollow sites, with one H atom in the hydroxy group pointing down. The surface energy of the Hdown configuration is lower than that of the H-up one by 1.79 meV/ $Å^2$. For the fully hydroxylated (1×1) surface, water molecules in the FAWL have strong interactions with the surface hydroxyl groups (659.8 meV/molecule) [104], comparable to the HB strength between water molecules in bulk Ice-XI (~710 meV/molecule in DFT [105] and ~610 meV/molecule in experiment [30]). This makes the monolayer water show a H-down configuration so that each water molecule in the FAWL can form one HB with the surface hydroxyl group.

3.3. Water at MgO surfaces

Compared to other binary metal oxides, the alkaline earth oxides have relatively simple rock-salt structure and electronic simplicity. Therefore, increasing research interest has been paid to the interactions between water molecules and the alkaline earth oxides, including MgO, CaO, BaO, and SrO [34, 35, 84, 106-114]. Previous LEED and IR study by Heidberg et al. [34] showed that there forms an ordered monolayer water on MgO(100) surface with a $c(4\times2)$ translational symmetry at 150 K, and water molecules in the FAWL are nearly parallel to the surface. Similar results have also been observed by Ferry et al. [35] via a combination of LEED and HAS. Also, they reported a transition from $c(4\times2)$ phase to a new $p(3\times2)$ phase at a temperature of 185 K. Since then, numerous theoretical studies have been carried out to investigate the adsorption structure of water monolayer with both $c(4\times2)$ and $p(3\times2)$ phases on MgO surface. Giordano and coworkers [113] employed DFT calculations to model the experimentally observed (3×2) water monolayer on MgO (100) surface, and they found that two out of six water molecules per unit cell dissociated, with two protons transferring to the neighboring surface oxygen sites. In addition, those intact water molecules tend to deviate from the atop adsorption sites and move close to the dissociated water molecules. Similarly, Cho et al. [114] determined the atomic arrangements of water monolayer with p (3×2) and c(4×2) phases on MgO(001) surface and demonstrated a mixed molecular and dissociative adsorption structure

Table 3. A summary of the surface model, adsorption state, coverage, and characterisation method for the FAWL on TiO2, SiO2, and MgO surfaces.

System	Surface	Adsorption state	Coverage (ML)	Characterisation	Reference
TiO ₂	Rutile(110)	Molecular	1	DFT	[90]
	Rutile(110)	Dissociative	1/8	DFT	[90]
	Rutile(100)	Molecular		IR	[91]
	Rutile(011)	Dissociative		DFT	[93]
	Anatase(001)	Dissociative	1/4	DFT	[96]
	Anatase(001)	Molecular	1	DFT	[96]
	Anatase(101)	Dissociative	1	DFT	[98, 99]
	Anatase(100)	Dissociative	1	DFT	[8]
SiO ₂	α-quartz (0001)	Molecular	1	DFT	[102, 104]
MgŌ	MgO(100)	Molecular (c(4 \times 2))		LEED, IR, HAS	[34]
	MgO(100)	Molecular $(p(3\times2))$		LEED, HAS	[35]
	MgO(100)	Dissociative $(p(3\times2))$		DFT	[113]
	MgO(001)	Dissociative		DFT	[114]
	MgO(001)	Dissociative ($c(4\times2)$)		XPS, DFT	[109]
	MgO(001)	Dissociative $(p(3\times2))$		XPS, DFT	[109]

for both phases. Meanwhile, the calculated adsorption energy for the $p(3\times2)$ water monolayer is 0.59 eV, slightly lower than that for the $c(4\times2)$ water monolayer (0.61 eV). Recently, a combined study from experiment and calculation by Wzodarczyk et al. [109] predicted that the $c(4\times2)$ structure, with ten water molecules per unit cell, is stable at low-temperature (see Figure 8(a)). However, at high temperature, the structure comprised of six water molecules per unit cell with $p(3\times2)$ structure is the most stable phase (see Figure 8(b)). Besides, they also noted that, in both stable structures, two water molecules in the FAWL undergo a partial dissociation, with the protons transferring to MgO surface and forming surface hydroxyl groups, as shown in Figure 8(a,b).

For water molecules on metal oxide surfaces, the adsorption state of the FAWL is highly dependent on the surface chemistry of the substrate. It is known that metal oxide surfaces contain unsaturated metal sites, which are preferential sites for water adsorption. Accordingly, the interaction strength between metal site and O atoms of water would determine the adsorption state of FAWL. On TiO₂ and MgO surfaces, part of the water molecules would partially dissociate after adsorption, whereas most water molecules exhibit molecular adsorption on SiO2 surface. However, it is worthwhile to mention that, when the SiO₂ surface is hydroxylated, the location of O atoms and the orientation of H atoms in the FAWL will change significantly to form well-defined HB networks. On the other hand, Table 3 illustrates that the water coverage plays a key role in the adsorption state of water molecules on TiO₂ surfaces. For example, water on rutile(110) surface prefers the dissociative adsorption at a low coverage, but the molecular adsorption at full coverage [90]. Water on MgO (100) surface also shows both molecular and dissociative adsorptions. Yet, only dissociative adsorption is observed for water at the MgO (001) surface. Meanwhile, the temperature increase could trigger the structural transition from $c(4\times2)$ to $p(3\times2)$ at MgO (100) and (001) surfaces, which affects the properties of FAWL accordingly [35, 109].

4. The properties of FAWL and their effects on other water molecules

Based on above discussions, it is accepted that the structures of FAWL on solid surfaces are the balanced results of water-

substrate and water-water interactions, indicating that the physical and chemical properties of FAWL can be remarkedly altered by the solid substrate. In this context, substantial strategies, including coating [115–117], roughness [18, 19, 118–121], curvature [122], morphology [123–125], and strain [126–128], have been proposed to regulate the interactions at the water—solid interface. Distinct scenarios have been observed for the FAWL on various solid surfaces, including wetting phenomena [122–126, 129–131], ice nucleation [1, 7, 18, 19, 40, 60, 132, 133], and low friction [134–136]. In this section, we mainly focus on the properties of FAWL and their effects on the other water molecules above the FAWL on solid surfaces.

4.1. The wetting property of FAWL

Experimentally, by using X-ray and neutron reflectometry, as well as AFM, James et al. [130] investigated the nanoscale condensation of water on self-assembled monolayers (SAMs) with the terminal of COOH groups. They observed that the SAMs surface is fully covered by a dense and continuous monolayer water with a thickness of 5.7Å, together with some small nanoscale water droplets above the monolayer water. Such a 'FAWL + water droplet' configuration has also been reported by CMD simulations on other solid surfaces, including metal [122, 124, 126, 131], metal oxide [137], talc [138], and ionic substrate [129]. For example, our recent study [126] showed that there exists an ordered monolayer water on both Pd (100) and Au (100) surfaces, but there is a big difference in the wettability between them. The FAWL on Pd (100) surface can stabilise a water droplet, whereas, on Au (100) surface, the FAWL is coved by a water film. Besides, we noted that, when a compressive strain from 0% to 5% is applied on the solid substrate, the FAWL on these two surfaces undergo an interesting wettability transition. In specific, when the strain is within 4% for Pd (100) surface, there exists a stable water droplet on the FAWL. However, when the strain was increased to 5%, a hydrophobic to hydrophilic wettability transition occurs (see Figure 9). For Au (100) surface, when the strain is within 1%, the FAWL on the surface is still coved by a water film. However, when the strain increases from 2% to 5%, water molecules in the film accumulate to form a water droplet (see Figure 9). Our analysis results revealed that, for the hydrophobic FAWL on both Pd (100) and Au (100) surfaces, there is a good match between

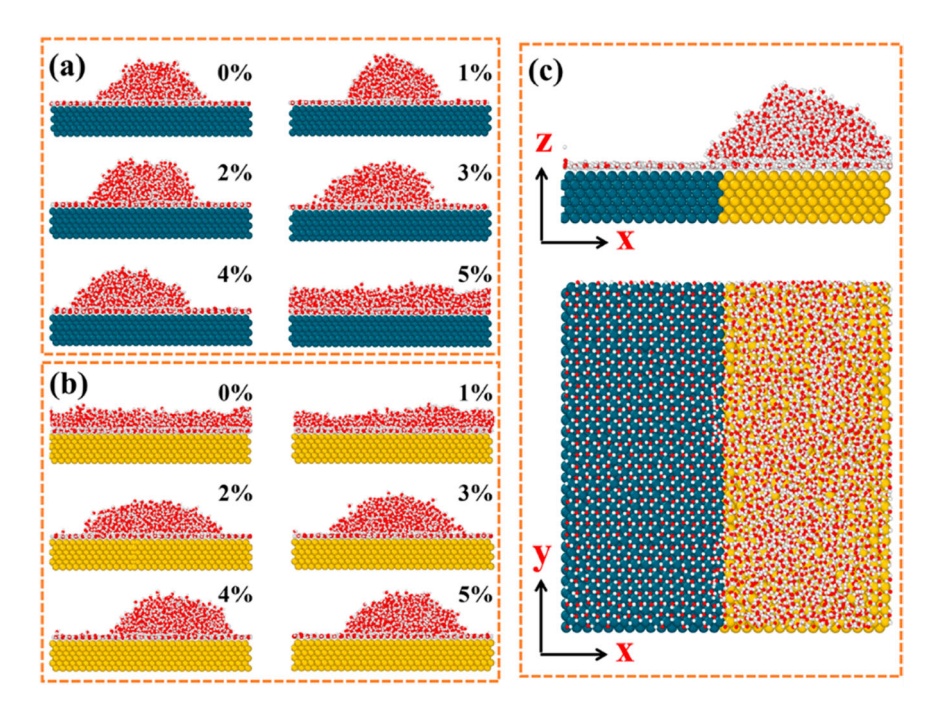


Figure 9. (Colour online) Equilibrium configurations of a 1.0 nm water film on metal surfaces under compressive strains: (a) Pd(100) and (b) Au(100); (c) top and side views of equilibrium structure on the bimetallic surface, where a water droplet is on the top of the compressive Au(100) region. Reproduced with permission from Ref. [126]. Copyright (2020) American Chemical Society.

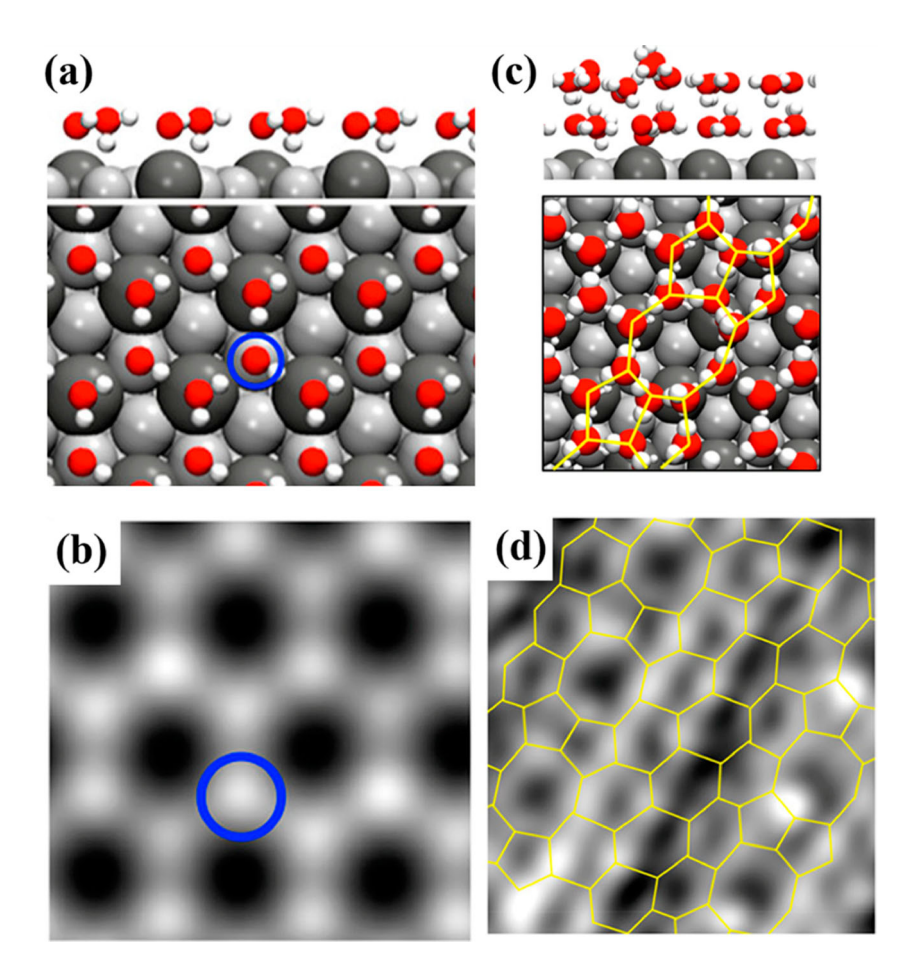


Figure 10. (Colour online) (a, c) Calculated structures and (b, d) STM images for the monolayer water and bilayer water, respectively, on the SnPt(111) surface. The blue circles in (a) and (b) represent the H-down sites. Reproduced with permission from Ref. [133]. Copyright (2019) American Chemical Society.



the lattice constant and the average water-water (O-O) distance of the FAWL. This contributes to an increase in average HB number within the FAWL and a more stable HB network. On the contrary, for the hydrophilic FAWL on both Pd (100) and Au (100) surfaces, the mismatch between the O-O distance and the lattice constant results in the FAWL structure much more easily being disturbed by water molecules present above the FAWL. Therefore, it is difficult for them to form a water droplet on the FAWL. Moreover, we also studied the water behaviours on bimetallic Pd(100) /Au(100) surface, where there is a monoaxially compressive strain of 4.61% on Au(100) surface along the Y direction to match lattice constants. Expectedly, we discovered an ordered FAWL on the bimetallic surface, but it is surprising to find that a water droplet is located on the compressed Au(100) region, while there is almost no water molecule left atop of the FAWL of the pristine Pd(100). This is mainly because there exists a big difference in orderliness and stability for the FAWL on both Pd (100) and Au (100) surfaces, which would trigger the migration of water molecules above the FAWL from Pd (100) to Au (100) surface.

4.2. The ice nucleating property of FAWL

On the other hand, extensive studies from experiments and calculations have also been dedicated to understanding the influence of surface morphology, hydrophobicity, and roughness on the ice nucleation [1, 7, 18, 19, 40, 60, 132, 133]. The MD simulations by Fitzner et al. [132] pointed out that the lattice match of solid substrate with respect to bulk ice is at most desirable but not a requirement. Instead, the balance between surface morphology and its hydrophobicity can significantly alter the ice nucleation rate. Besides, the experiment studies by Hodgson and coworkers [18, 19] reported that, on stepped Cu(511) surface, water molecules can form extended 2D buckled hexagonal wetting layer. Such water overlayer contains hydrogen donor and acceptor sites to make the second water layer adsorb on top of the FAWL and thereby form a commensurate ice film. They also demonstrated that the resulted multilayer ice is stabilised by the relaxation of the corrugation and H orientation of water molecules in the FAWL. This can produce Hdonor and H-acceptor sites at next nearest neighbor positions around the water hexagons, mimicking the arrangement in bulk ice Ih(0001) [18, 19]. Furthermore, they also investigated the ice growth on a SnPt(111) template with a lattice spacing 6% larger than ice, by using STM and DFT calculations. They found that the FAWL can form a strictly commensurate hexagonal network, but this structure is not beneficial for the adsorption of the second water layer due to the absence of Hup water molecules in the FAWL (see Figure 10(a,b)) [133]. Instead, when water molecules in the FAWL forms a 2D structure containing extended defect rows comprised of pentamer and octamer rings linked by the hexagonal water molecules (see Figure 10(c,d)), it would promote the growth of the second water layer and allow it to keep commensurate structure with the FAWL. Recently, Zhu et al. [60] performed the CMD simulations to investigate the growth of 2D ice on various solid surfaces with a series of water adsorption energies and lattice parameters. They found that the transition from liquid water

to bilayer hexagonal ice can happen on solid surfaces near room temperature without nanoscale confinement. Moreover, they noted that the liquid-to-bilayer transition can occur only when the water-surface interaction parameter is larger than a critical value [60]. Unexpectedly, such 2D ice has been detected on Au (111) surface by Jiang and coworkers [40] via the noncontact AFM experiment coupled with the CMD and DFT calculations. Their results further revealed that the 2D ice grown on Au(111) surface corresponds to an interlocked bilayer ice structure making from two flat hexagonal water layers. In each layer, half of the water molecules prefer the orientation parallel to the surface and the other half tend to be perpendicular to the surface, with one O-H either upward or downward.

5. Summary and outlook

Herein, we give an overview of experimental and theoretical insights into the adsorption structures of FAWL on solid substrates. These studies have demonstrated that water adsorption at the interface is very complicated and sensitive to the structure and chemistry of individual surface. Experimentally, low temperature STM measurements are capable of providing atomic-level images of water in the FAWL, enabling us to make a direct comparison with the results from theoretical calculations. Besides, other surface science techniques like LEED can detect the ordering of thin water film on the surface, while XPS/XAS can provide useful information to distinguish molecular and dissociate adsorption. Indeed, the adsorption state of water molecules on solid surfaces is largely influenced by the temperature, coverage, and surface geometry.

For the adsorption structure on Ru(0001) surface, an intact water overlayer was observed when the temperature is below 155 K. Upon increasing the temperature to be 180 K, the FAWL would undergo a partial dissociation to generate a stable H₂O-OH phase [11]. The DFT calculations showed that mixed OH/H₂O structure is much more energetically favourable over the intact water overlayer [57,58]. On the other hand, early LEED results proposed that the water overlayer on Pt(111) surface exhibits a $(\sqrt{3} \times \sqrt{3})R30^{\circ}$ structure. However, later studies suggested a $(\sqrt{37} \times \sqrt{37})R25.3^{\circ}$ structure for the FAWL at sub-monolayer coverage, and then it would change to $(\sqrt{39} \times \sqrt{39})R16.1^{\circ}$ structure when the coverage is at saturation. Among these three structures, the DFT calculations showed an adsorption energy of 597 and 615 meV for $(\sqrt{37} \times \sqrt{37})R25.3^{\circ}$ and $(\sqrt{39} \times \sqrt{39})R16.1^{\circ}$ phases, respectively, compared to a corresponding value of 534 meV for the commensurate $(\sqrt{3} \times \sqrt{3})R30^{\circ}$ phase. Different from a complete water overlayer on Ru(0001) and Pt(111) surfaces, water molecules on stepped Pt surface form 1D or 2D chain, which contains different water rings. Moreover, it is interesting to find that the step-in substrate is beneficial for the formation of 1D water chain, while the terrace is important for the formation of 2D water networks.

Similarly, the adsorption structures of water molecules on metal oxide surfaces are closely related to the characteristics of exposed surfaces. The topmost of these oxide surfaces always contain under-coordinated metal and oxygen sites, which determines the surface reactivity for the water dissociation. Typically, water molecules can adsorb above the metal sites via oxygen lone pair and form HB with the readily available surface lattice oxygen atoms. The interaction strength of water-metal and HB would significantly influence the dissociation of water molecules. Yet, we want to point out that the water coverage also plays a key role in water dissociation. Prior studies showed that, for rutile (110) surface, an intact water structure is observed at a full monolayer coverage, whereas a mixed hydroxyl/water structure is observed at a low coverage (e.g. 1/8 monolayer) [79]. However, for hydroxylated α-quartz (0001) surface, there is no dissociation for water molecules in the FAWL, and coverage variation only affects the water orientation to form HBs with surface hydroxyls.

Upon the adsorption of FAWL on metal surfaces, their structures and properties can have a profound influence on multilayer ice nucleation and wetting behaviour. When there is a good match between the lattice constant and the average water-water distance of FAWL, it would generate strong water-metal and in-plane HB interactions that enable the formation of ordered FAWL. Such ordered monolayer water would reduce the possibility to form HB between the first and second water layer, leading to the generation of a water droplet above the FAWL. Therefore, forming strong HBs is necessary for multilayer water adsorption to wet the FAWL. It is proposed that the strong HBs are formed only when the FAWL contains free OH groups [3]. These groups can act as HB donor for water molecules above the FAWL, which is one of the prerequisites for ice nucleation. Aside from that, another important factor is that ice nucleation requires the FAWL to have a suitable lateral arrangement to match the structure in bulk ice Ih [3].

Till now, tremendous progress has been obtained, via a combination of experiments and calculations, in understanding the adsorption, dissociation, diffusion, and nucleation of liquid water on metal and oxide surfaces over the past decades. However, there still exists some problems and challenges in investigating the water behaviours on solid surfaces. For the experiments, most high-resolution techniques require to be operated under extreme environment of ultra-high vacuum and low temperature. In this case, the solid water structure is completely different from the liquid water at ambient conditions. Therefore, it is still challenging but critical to use high-resolution techniques to probe the structure and properties of liquid water, due to its great importance to our human beings' daily life. In addition, it is also urgent to have detailed insights into the interactions between water and other novel materials, such as biomaterials [139], polymers [140], and graphene-based materials [141, 142]. Progress in this area would promote their extensive applications in drug delivery, biosensing, water separation/purification, and anticorrosion. Wherein, a number of studies are needed to explore the adsorption and diffusion within graphene oxide (GO) membrane since a better understanding in this direction can help to optimise the membrane performance. Besides, recent studies have shown that the graphene-based 2D materials are capable of protecting metal substrate from corrosion [143], but little is known about underlying mechanisms and how intrinsic defects influence its anticorrosion capacity. Therefore, great efforts are also needed in this area to extend potential application of graphene-based materials in anticorrosion field.

For the adsorption of water molecules on the substrate, the HB interaction is an important interaction to stabilise the FAWL at solid interfaces, however, an accurate description of the HB is still challenging for theoretical studies. When water molecules approach the solid surface, the local electric field from the substrate will disturb the electron distribution of H atoms and such polarisation interaction may induce the electron transfer from the H to the substrate [3]. However, for MD simulations with classical force field, it is insufficient to describe such process due to the fact that the partial charge of the classical force field is a fixed value for each atom. In addition, for both reactive force field and classical force field, they fail to adequately account for the quantum effect for the H nuclei, which would significantly influence the HB networks and dynamics [144-146]. This is mainly due to that the nonharmonic quantum fluctuations of H nuclei will change the OH bond length in water molecule and HB angle, which in turn affects the bond energy and configuration of the HB [144]. Although great efforts have been devoted to investigating the issue of quantum fluctuations [147-149], it is still unclear how the quantum effect of H nuclei will exactly affect the HB formation and dynamics. On the other hand, it has been reported that the HB plays a critical role in catalytic reactions, protein folding, molecular self-assembly, gas separation, and proton transfer, from simple to complex systems. Therefore, it is still of great challenges to quantitively determine the properties of HB, when a very similar set of criteria is adopted to probe HBs of those different systems. There is a lack of an adjustable parameter to connect the HB to the complexity of systems. It is also worth pointing out that despite the feasibility of obtaining the vibrational spectroscopy information from experiments, the direct experimental measurement of HBs is rarely reported. While computational studies can acquire both vibrational spectroscopy and HB information, it would be useful to experimentally determine the complex HB network at the liquid-solid interface and combine theoretical studies to construct a relationship between the vibrational information and the microscopic HB properties [150-153].

On the other hand, theoretical studies, including Monte Carlo (MC) method, molecular dynamics (MD) simulation, and DFT calculations, have been extensively employed to predict diverse properties of distinct liquid-solid interfaces. However, there are still two main bottlenecks that may hinder the fundamental understanding of water at interface: (1) a computationally inexpensive method to simulate the atomic model representative of the realistic system which contains thousands to millions of atoms; (2) the atomic interactions predicted in the model should adequately represent quantum-mechanical interactions of the system [154]. In this context, developing efficient and reliable atomic potentials to gain the in-depth understanding of complex liquid-solid interface systems has received tremendous attentions over the past years [154–165]. Recently, the machine-learning potential (MLP) provides another choice to reproduce DFT calculations and enable a satisfactory description of complex systems. Unlike traditional classical force fields with specific functional forms, the MLPs have flexible functional forms and the parameters are based on a large number of training data from DFT calculations. Promising progresses have been available in the construction



of MLPs for systems including bulk materials [156], metal surface [157], metal alloy [158], aqueous electrolyte solutions [159], bulk water, and liquid-solid interface [155, 161–163]. For example, Natarajan and Behler [161] constructed a DFTbased neutral network potential to study the properties of interfacial water at Cu(111), Cu(100), and Cu(110) surfaces. They found that the water molecules in the first hydration layer at all three interfaces tend to locate at the atop sites and are organised to parallel to the surface. Those in the second layer prefer the more tilted configurations and show a significant difference in the spatial arrangement. Developing force fields via machine learning algorithms is certainly an exciting research direction, efforts are strongly encouraged to promote the application of MLPs in complex interfacial systems.

Acknowledgements

We acknowledge the U.S. National Science Foundation (NSF) for support through the grant CHE-1710102. L.H. also gratefully acknowledges DTRA for the financial support (grant HDTRA11910008). We are very pleased to thank the OU Supercomputing Center for Education & Research (OSCER) at University of Oklahoma for computational resources and dedicated support.

Disclosure statement

No potential conflict of interest was reported by the author(s).

Funding

This work was supported by National Science Foundation [grant number CHE-1710102] and DTRA [grant number HDTRA11910008].

References

- [1] Bjornehohn E, Hansen MH, Hodgson A, et al. Water at interfaces. Chem Rev. 2016;116:7698-7726.
- [2] Mu RT, Zhao ZJ, Dohnalek Z, et al. Structural motifs of water on metal oxide surfaces. Chem Soc Rev. 2017;46:1785-1806.
- [3] Hodgson A, Haq S. Water adsorption and the wetting of metal surfaces. Surf Sci Rep. 2009;64:381-451.
- [4] Fujishima A, Honda K. Electrochemical photolysis of water at a semiconductor electrode. Nature. 1972;238:37-38.
- [5] Maier S, Salmeron M. How does water wet a surface? Acc Chem Res. 2015;48:2783-2790.
- [6] Shimizu TK, Maier S, Verdaguer A, et al. Water at surfaces and interfaces: from molecules to ice and bulk liquid. Prog Surf Sci. 2018;93:87-107.
- [7] Carrasco J, Hodgson A, Michaelides A. A molecular perspective of water at metal interfaces. Nat Mater. 2012;11:667-674.
- [8] Sun CH, Liu LM, Selloni A, et al. Titania-water interactions: a review of theoretical studies. J Mater Chem. 2010;20:10319-10334.
- [9] Rimola A, Costa D, Sodupe M, et al. Silica surface features and their role in the adsorption of biomolecules: computational modeling and experiments. Chem Rev. 2013;113:4216-4313.
- [10] Lanzani G, Martinazzo R, Materzanini G, et al. Chemistry at surfaces: from ab initio structures to quantum dynamics. Theor Chem Acc. 2007;117:805-825.
- [11] Tatarkhanov M, Fomin E, Salmeron M, et al. The structure of mixed H2O-OH monolayer films on Ru(0001). J Chem Phys. 2008:129:154109.
- [12] Maier S, Lechner BAJ, Somorjai GA, et al. Growth and structure of the first layers of ice on Ru(0001) and Pt(111). J Am Chem Soc. 2016;138:3145-3151.

- [13] Morgenstern M, Muller J, Michely T, et al. The ice bilayer on Pt (111): nucleation, structure and melting. Z Phys Chem. 1997:198:43-72
- [14] Nie S, Feibelman PJ, Bartelt NC, et al. Pentagons and heptagons in the first water layer on Pt(111). Phys Rev Lett. 2010;105:026102.
- [15] Feibelman PJ, Bartelt NC, Nie S, et al. Interpretation of high-resolution images of the best-bound wetting layers on Pt(111). J Chem Phys. 2010;133:154703.
- [16] Standop S, Redinger A, Morgenstern M, et al. Molecular structure of the H₂O wetting layer on Pt(111). Phys Rev B. 2010;82:161412.
- [17] Standop S, Morgenstern M, Michely T, et al. H20 on Pt(111): structure and stability of the first wetting layer. J Phys: Condens Matter. 2012;24:124103.
- [18] Lin CF, Corem G, Godsi O, et al. Ice nucleation on a corrugated surface. J Am Chem Soc. 2018;140:15804-15811.
- [19] Lin C, Avidor N, Corem G, et al. Two-dimensional wetting of a stepped copper surface. Phys Rev Lett. 2018;120:076101.
- [20] Kolb MJ, Farber RG, Derouin J, et al. Double-stranded water on stepped platinum surfaces. Phys Rev Lett. 2016;116:136101.
- [21] Peng JB, Guo J, Hapala P, et al. Weakly perturbative imaging of interfacial water with submolecular resolution by atomic force microscopy. Nat Commun. 2018;9:122.
- Shiotari A, Sugimoto Y. Ultrahigh-resolution imaging of water networks by atomic force microscopy. Nat Commun. 2017;8:14313.
- [23] Weissenrieder J, Mikkelsen A, Andersen JN, et al. Experimental evidence for a partially dissociated water bilayer on Ru{0001}. Phys Rev Lett. 2004;93:196102.
- [24] Ogasawara H, Brena B, Nordlund D, et al. Structure and bonding of water on Pt(111). Phys Rev Lett. 2002;89:276102.
- [25] Schaefer A, Lanzilotto V, Cappel U, et al. First layer water phases on anatase TiO2(101). Surf Sci. 2018;674:25-31.
- [26] Kim Y, Shin S, Moon ES, et al. Spectroscopic monitoring of the acidity of water films on Ru(0001): orientation-specific acidity of adsorbed water. Chem-Eur J. 2014;20:3376-3383.
- [27] Su XC, Lianos L, Shen YR, et al. Surface-induced ferroelectric ice on Pt(111). Phys Rev Lett. 1998;80:1533-1536.
- [28] Thiel PA, Hoffmann FM, Weinberg WH. Monolayer and multilayer adsorption of water on Ru(001). J Chem Phys. 1981;75:5556-5572.
- [29] Held G, Menzel D. The structure of the bilayer of D2O on Ru(001). Surf Sci. 1994;316:92-102.
- Feibelman PJ. Partial dissociation of water on Ru(0001). Science. 2002;295:99-102.
- [31] Firment LE, Somorjai GA. Surface-structures of vapor-grown ice and naphthalene crystals studied by low-energy electron-diffraction. Surf Sci. 1976;55:413-426.
- [32] Haq S, Harnett J, Hodgson A. Growth of thin crystalline ice films on Pt(111). Surf Sci. 2002;505:171-182.
- [33] Harnett J, Haq S, Hodgson A. Electron induced restructuring of crystalline ice adsorbed on Pt(111). Surf Sci. 2003;528:15-19.
- [34] Heidberg J, Redlich B, Wetter D. Adsorption of water-vapor on the MgO(100) single-crystal surface. Ber Bunsen Phys Chem. 1995;99:1333-1337.
- [35] Ferry D, Glebov A, Senz V, et al. Observation of the second ordered phase of water on the MgO(100) surface: Low energy electron diffraction and helium atom scattering studies. J Chem Phys. 1996;105:1697-1701.
- [36] Glebov A, Graham AP, Menzel A, et al. Orientational ordering of two-dimensional ice on Pt(111). J Chem Phys. 1997;106:9382-9385.
- Gawronski H, Carrasco J, Michaelides A, et al. Manipulation and control of hydrogen bond dynamics in absorbed ice nanoclusters. Phys Rev Lett. 2008;101:136102.
- [38] Mehlhorn M, Gawronski H, Morgenstern K. Electron damage to supported ice investigated by scanning tunneling microscopy and spectroscopy. Phys Rev Lett. 2008;101:196101.
- [39] Cavalleri M, Ogasawara H, Pettersson LGM, et al. The interpretation of x-ray absorption spectra of water and ice. Chem Phys Lett. 2002;364:363-370.



- [40] Ma RZ, Cao DY, Zhu CQ, et al. Atomic imaging of the edge structure and growth of a two-dimensional hexagonal ice. Nature. 2020;577:60-63.
- [41] Gillan MJ, Alfe D, Michaelides A. Perspective: How good is DFT for water? J Chem Phys. 2016;144:130901.
- Hamann DR. H2o hydrogen bonding in density-functional theory. Phys Rev B. 1997;55:10157-10160.
- Hamada I, Lee K, Morikawa Y. Interaction of water with a metal surface: importance of van der waals forces. Phys Rev B. 2010:81:115452.
- [44] Carrasco J, Klimes J, Michaelides A. The role of van der waals forces in water adsorption on metals. J Chem Phys. 2013;138:024708.
- [45] Carrasco J, Santra B, Klimes J, et al. To wet or not to wet? Dispersion forces tip the balance for water ice on metals. Phys Rev Lett. 2011;106:026101.
- [46] Tonigold K, Gross A. Dispersive interactions in water bilayers at metallic surfaces: A comparison of the PBE and rPBE functional including semiempirical dispersion corrections. J Comput Chem. 2012;33:695-701.
- [47] Zhou G, Liu C, Bumm LA, et al. Force field parameter development for the thiolate/defective au (111) interface. Langmuir. 2020;15:4098-4107.
- [48] Senftle TP, Hong S, Islam MM, et al. The reaxff reactive force-field: development, applications and future directions. NPJ Comput Mater. 2016;2:15011.
- [49] Huang LL, Gubbins KE, Li LC, et al. Water on titanium dioxide surface: A revisiting by reactive molecular dynamics simulations. Langmuir. 2014;30:14832-14840.
- [50] Kim SY, Kumar N, Persson P, et al. Development of a reaxff reactive force field for titanium dioxide/water systems. Langmuir. 2013;29:7838-7846.
- [51] Raymand D, van Duin ACT, Spangberg D, et al. Water adsorption on stepped zno surfaces from md simulation. Surf Sci. 2010;604:741-752.
- [52] Fogarty JC, Aktulga HM, Grama AY, et al. A reactive molecular dynamics simulation of the silica-water interface. J Chem Phys. 2010;132:174704.
- [53] Wen JL, Ma TB, Zhang WW, et al. Surface orientation and temperature effects on the interaction of silicon with water: molecular dynamics simulations using reaxff reactive force field. J Phys Chem A. 2017;121:587-594.
- [54] Ai LQ, Zhou YS, Huang HS, et al. A reactive force field molecular dynamics simulation of nickel oxidation in supercritical water. J Supercrit Fluids. 2018;133:421-428.
- [55] van Duin ACT, Bryantsev VS, Diallo MS, et al. Development and validation of a reaxff reactive force field for cu cation/water interactions and copper metal/metal oxide/metal hydroxide condensed phases. J Phys Chem A. 2010;114:9507-9514.
- [56] Kim SY, van Duin ACT. Simulation of titanium metal/titanium dioxide etching with chlorine and hydrogen chloride gases using the reaxff reactive force field. J Phys Chem A. 2013;117:5655-5663.
- [57] Berg A, Peter C, Johnston K. Evaluation and optimization of interface force fields for water on gold surfaces. J Chem Theory Comput. 2017;13:5610-5623.
- [58] Bandura AV, Sykes DG, Kubicki JD. Derivation of force field parameters for TiO2-H2O systems from ab initio calculations. J Phys Chem B. 2003;107:11072-11081.
- [59] Clabaut P, Fleurat-Lessard P, Michel C, et al. Ten facets, one force field: The gal19 force field for water-noble metal interfaces. J Chem Theory Comput. 2020. DOI:10.1021/acs.jctc.1020c00091
- Zhu CO, Gao YR, Zhu WD, et al. Direct observation of 2dimensional ices on different surfaces near room temperature without confinement. Proc Natl Acad Sci USA. 2019;116:16723-
- [61] Luan BQ, Huynh T, Zhou RH. Simplified TiO2 force fields for studies of its interaction with biomolecules. J Chem Phys. 2015;142:234102.
- [62] Vega C, Abascal JLF. Simulating water with rigid non-polarizable models: A general perspective. Phys Chem Chem Phys. 2011;13:19663-19688.

- [63] Abascal JLF, Vega C. A general purpose model for the condensed phases of water: TIP4P/2005. J Chem Phys. 2005;123:234505.
- [64] Abascal JLF, Sanz E, Fernandez RG, et al. A potential model for the study of ices and amorphous water: TIP4P/Ice. J Chem Phys. 2005;122:234511.
- [65] McBride F, Hodgson A. Water and its partially dissociated fragments at metal surfaces. Int Rev Phys Chem. 2017;36:1-38.
- Thiel PA, Madey TE. The interaction of water with solid surfaces: fundamental aspects. Surf Sci Rep. 1987;7:211-385.
- Forster M, Raval R, Hodgson A, et al. C(2(2) water-hydroxyl layer on Cu(110): A wetting layer stabilized by bjerrum defects. Phys Rev Lett. 2011;106:046103.
- [68] Michaelides A, Alavi A, King DA. Different surface chemistries of water on Ru{0001}: from monomer adsorption to partially dissociated bilayers. J Am Chem Soc. 2003;125:2746-2755.
- [69] Messaoudi S, Dhouib A, Abderrabba M, et al. Wetting of intact and partially dissociated water layer on Ru(0001): A density functional study. J Phys Chem C. 2011;115:5834-5840.
- Tatarkhanov M, Ogletree DF, Rose F, et al. Metal- and hydrogenbonding competition during water adsorption on Pd(111) and Ru (0001). J Am Chem Soc. 2009;131:18425-18434.
- [71] Hamada I, Meng S. Water wetting on representative metal surfaces: improved description from van der waals density functionals. Chem Phys Lett. 2012;521:161-166.
- [72] Meng S, Xu LF, Wang EG, et al. Vibrational recognition of hydrogen-bonded water networks on a metal surface. Phys Rev Lett. 2002;89:176104.
- [73] Meng S, Wang EG, Gao SW. Water adsorption on metal surfaces: A general picture from density functional theory studies. Phys Rev B. 2004:69:195404.
- [74] Michaelides A, Ranea VA, de Andres PL, et al. General model for water monomer adsorption on close-packed transition and noble metal surfaces. Phys Rev Lett. 2003;90:216102.
- [75] Meng S. Dynamical properties and the proton transfer mechanism in the wetting water layer on Pt(111). Surf Sci. 2005;575:300-306.
- [76] Bu YF, Cui TT, Zhao M, et al. Evolution of water structures on stepped platinum surfaces. J Phys Chem C. 2018;122:604-611.
- [77] Pekoz R, Donadio D. Dissociative adsorption of water at (211) stepped metallic surfaces by first-principles simulations. J Phys Chem C. 2017;121:16783-16791.
- [78] Donadio D, Ghiringhelli LM, Delle Site L. Autocatalytic and cooperatively stabilized dissociation of water on a stepped platinum surface. J Am Chem Soc. 2012;134:19217-19222.
- Kolb MJ, Wermink J, Calle-Vallejo F, et al. Initial stages of water solvation of stepped platinum surfaces. Phys Chem Chem Phys. 2016;18:3416-3422.
- [80] Lin XH, Gross A. First-principles study of the water structure on flat and stepped gold surfaces. Surf Sci. 2012;606:886-891.
- [81] Nakamura M, Sato N, Hoshi N, et al. One-dimensional zigzag chain of water formed on a stepped surface. J Phys Chem C. 2009;113:4538-4542.
- Endo O, Nakamura M, Sumii R, et al. 1d hydrogen bond chain on Pt(211) stepped surface observed by o k-nexafs spectroscopy. J Phys Chem C. 2012;116:13980-13984.
- [83] Pekoz R, Worner S, Ghiringhelli LM, et al. Trends in the adsorption and dissociation of water clusters on flat and stepped metallic surfaces. J Phys Chem C. 2014;118:29990-29998.
- [84] Sterrer M, Nilius N, Shaikhutdinov S, et al. Interaction of water with oxide thin film model systems. J Mater Res. 2019;34:360-378.
- Yang JJ, Wang EG. Reaction of water on silica surfaces. Curr Opin Solid St M. 2006;10:33-39.
- Bai J, Zhou BX. Titanium dioxide nanomaterials for sensor applications. Chem Rev. 2014;114:10131-10176.
- Kapilashrami M, Zhang YF, Liu YS, et al. Probing the optical property and electronic structure of tio2 nanomaterials for renewable energy applications. Chem Rev. 2014;114:9662-9707.
- [88] Rajh T, Dimitrijevic NM, Bissonnette M, et al. Titanium dioxide in the service of the biomedical revolution. Chem Rev. 2014;114:10177-10216.



- [89] Raju M, Kim SY, van Duin ACT, et al. Reaxff reactive force field study of the dissociation of water on titania surfaces. J Phys Chem C. 2013;117:10558-10572.
- [90] Kowalski PM, Meyer B, Marx D. Composition, structure, and stability of the rutile TiO2(110) surface: oxygen depletion, hydroxylation, hydrogen migration, and water adsorption. Phys Rev B. 2009;79:115410.
- [91] Suda Y, Morimoto T. Molecularly adsorbed H2O on the bare surface of TiO2 (rutile). Langmuir. 1987;3:786-788.
- [92] Diebold U. The surface science of titanium dioxide. Surf Sci Rep. 2003;48:53-229.
- [93] Barnard AS, Zapol P, Curtiss LA. Modeling the morphology and phase stability of TiO2 nanocrystals in water. J Chem Theory Comput. 2005;1:107-116.
- [94] Beck TJ, Klust A, Batzill M, et al. Surface structure of TiO2(011)-(2 (1). Phys Rev Lett. 2004;93:036104.
- [95] Di Valentin C, Tilocca A, Selloni A, et al. Adsorption of water on reconstructed rutile TiO2(011)-(2(1): Ti=O double bonds and surface reactivity. J Am Chem Soc. 2005;127:9895-9903.
- [96] Vittadini A, Selloni A, Rotzinger FP, et al. Structure and energetics of water adsorbed at TiO2 anatase (101) and (001) surfaces. Phys Rev Lett. 1998;81:2954-2957.
- [97] Selloni A, Vittadini A, Gratzel M. The adsorption of small molecules on the tio2 anatase(101) surface by first-principles molecular dynamics. Surf Sci. 1998;402:219-222.
- Patrick CE, Giustino F. Structure of a water monolayer on the anatase TiO2(101) surface. Phys Rev Appl. 2014;2:014001.
- Martinez-Casado R, Mallia G, Harrison NM, et al. First-principles study of the water adsorption on anatase(101) as a function of the coverage. J Phys Chem C. 2018;122:20736-20744.
- [100] Zhou GB, Liu C, Huang LL. Molecular dynamics simulation of firstadsorbed water layer at titanium dioxide surfaces. J Chem Eng Data. 2018;63:2420-2429.
- [101] Limo MJ, Sola-Rabada A, Boix E, et al. Interactions between metal oxides and biomolecules: from fundamental understanding to applications. Chem Rev. 2018;118:11118-11193.
- [102] Yang JJ, Wang EG. Water adsorption on hydroxylated alpha-quartz (0001) surfaces: from monomer to flat bilayer. Phys Rev B. 2006;73:035406.
- [103] Bampoulis P, Sotthewes K, Dollekamp E, et al. Water confined in two-dimensions: Fundamentals and applications. Surf Sci Rep. 2018;73:233-264.
- Chen YW, Chu IH, Wang Y, et al. Water thin film-silica interaction on alpha-quartz (0001) surfaces. Phys Rev B. 2011;84:155444.
- Pan D, Liu LM, Tribello GA, et al. Surface energy and surface proton order of ice ih. Phys Rev Lett. 2008;101:155703.
- [106] Oncak M, Wlodarczyk R, Sauer J. Hydration structures of MgO, CaO, and SrO (001) surfaces. J Phys Chem 2016;120:24762-24769.
- [107] Fujimori Y, Zhao XH, Shao X, et al. Interaction of water with the CaO(001) surface. J Phys Chem C. 2016;120:5565-5576.
- Foster M, D'Agostino M, Passno D. Water on MgO(100)-An infrared study at ambient temperatures. Surf Sci. 2005;590:31-41.
- [109] Wlodarczyk R, Sierka M, Kwapien K, et al. Structures of the ordered water monolayer on MgO(001). J Phys Chem C. 2011;115:6764-
- [110] Carrasco E, Aumer A, Gomes JF, et al. Vibrational spectroscopic observation of ice dewetting on MgO(001). Chem Commun. 2013;49:4355-4357.
- [111] Demirdjian B, Suzanne J, Ferry D, et al. Neutron diffraction investigation of water on MgO(001) surfaces, from monolayer to bulk condensation. Surf Sci. 2000;462:L581-L586.
- [112] Yu YH, Guo QL, Liu S, et al. Partial dissociation of water on a MgO (100) film. Phys Rev B. 2003;68:115414.
- [113] Giordano L, Goniakowski J, Suzanne J. Partial dissociation of water molecules in the (3(2)) water monolayer deposited on the MgO(100)surface. Phys Rev Lett. 1998;81:1271-1273.
- [114] Cho JH, Park JM, Kim KS. Influence of intermolecular hydrogen bonding on water dissociation at the MgO(001) surface. Phys Rev B. 2000;62:9981-9984.

- [115] Rafiee J, Mi X, Gullapalli H, et al. Wetting transparency of graphene. Nat Mater. 2012;11:217-222.
- [116] Andrews JE, Sinha S, Chung PW, et al. Wetting dynamics of a water nanodrop on graphene. Phys Chem Chem Phys. 2016;18:23482-23493.
- [117] Ashraf A, Wu YB, Wang MC, et al. Doping-induced tunable wettability and adhesion of graphene. Nano Lett. 2016;16:4708-4712.
- Yao X, Song YL, Jiang L. Applications of bio-inspired special wettable surfaces. Adv Mater. 2011;23:719-734.
- Zhang SN, Huang JY, Chen Z, et al. Bioinspired special wettability surfaces: from fundamental research to water harvesting applications. Small. 2017;13:1602992.
- Wang ZX, Elimelech M, Lin SH. Environmental applications of interfacial materials with special wettability. Environ Sci Technol. 2016;50:2132-2150.
- [121] Liu KS, Jiang L. Metallic surfaces with special wettability. Nanoscale. 2011;3:825-838.
- [122] Zhu Z, Guo HK, Jiang XK, et al. Reversible hydrophobicity-hydrophilicity transition modulated by surface curvature. J Phys Chem Lett. 2018;9:2346-2352.
- [123] Zhu CQ, Li H, Huang YF, et al. Microscopic insight into surface wetting: Relations between interfacial water structure and the underlying lattice constant. Phys Rev Lett. 2013;110:126101.
- [124] Xu Z, Gao Y, Wang CL, et al. Nanoscale hydrophilicity on metal surfaces at room temperature: Coupling lattice constants and crystal faces. J Phys Chem C. 2015;119:20409-20415.
- van der Niet MJTC, den Dunnen A, Koper MTM, et al. Tuning hydrophobicity of platinum by small changes in surface morphology. Phys Rev Lett. 2011;107:146103.
- [126] Zhou G, Schoen BH, Yang Z, et al. First adsorbed water layer and its wettability transition under compressive lattice strain. J Phys Chem C. 2020;124:4057-4064.
- [127] Zhang W, Ye C, Hong LB, et al. Molecular structure and dynamics of water on pristine and strained phosphorene: wetting and diffusion at nanoscale. Sci Rep. 2016;6:38327.
- [128] Chialvo AA, Vlcek L, Cummings PT. Surface strain effects on the water-graphene interfacial and confinement behavior. J Phys Chem C. 2014;118:19701-19711.
- [129] Wang CL, Lu HJ, Wang ZG, et al. Stable liquid water droplet on a water monolayer formed at room temperature on ionic model substrates. Phys Rev Lett. 2009;103:137801.
- [130] James M, Darwish TA, Ciampi S, et al. Nanoscale condensation of water on self-assembled monolayers. Soft Matter. 2011;7:5309-5318.
- [131] Limmer DT, Willard AP, Madden P, et al. Hydration of metal surfaces can be dynamically heterogeneous and hydrophobic. Proc Natl Acad Sci USA. 2013;110:4200-4205.
- [132] Fitzner M, Sosso GC, Cox SJ, et al. The many faces of heterogeneous ice nucleation: Interplay between surface morphology and hydrophobicity. J Am Chem Soc. 2015;137:13658-13669.
- Gerrard N, Gattinoni C, McBride F, et al. Strain relief during ice growth on a hexagonal template. J Am Chem Soc. 2019;141:8599-8607.
- [134] Yu XM, Qi CH, Wang CL. Enhancement of water self-diffusion at super-hydrophilic surface with ordered water. Chinese Phys B. 2018;27:060101.
- [135] Wang CL, Wen BH, Tu YS, et al. Friction reduction at a superhydrophilic surface: role of ordered water. J Phys Chem C. 2015;119:11679-11684.
- [136] Ho TA, Papavassiliou DV, Lee LL, et al. Liquid water can slip on a hydrophilic surface. Proc Natl Acad Sci USA. 2011;108:16170-16175.
- Phan A, Ho TA, Cole DR, et al. Molecular structure and dynamics [137] in thin water films at metal oxide surfaces: Magnesium, aluminum, and silicon oxide surfaces. J Phys Chem C. 2012;116:15962-15973.
- [138] Rotenberg B, Patel AJ, Chandler D. Molecular explanation for why talc surfaces can be both hydrophilic and hydrophobic. J Am Chem Soc. 2011;133:20521-20527.



- [139] Shao Q, Jiang SY. Molecular understanding and design of zwitterionic materials. Adv Mater. 2015;27:15-26.
- Buruga K, Song H, Shang J, et al. A review on functional polymerclay based nanocomposite membranes for treatment of water. J Hazard Mater. 2019;379:120584.
- Melios C, Giusca CE, Panchal V, et al. Water on graphene: review of recent progress. 2D Mater. 2018;5:022001.
- Wei Y, Zhang YS, Gao XL, et al. Multilayered graphene oxide membranes for water treatment: A review. Carbon N Y. 2018;139:964–981.
- [143] Cui G, Bi ZX, Zhang RY, et al. A comprehensive review on graphenebased anti-corrosive coatings. Chem Eng J. 2019;373:104-121.
- [144] Peng JB, Guo J, Jiang Y. Probing surface water at submolecular level with scanning probe microscopy. Sci Sin Chim. 2019;49:536–555.
- [145] McKenzie RH, Bekker C, Athokpam B, et al. Effect of quantum nuclear motion on hydrogen bonding. J Chem Phys. 2014;140:174508.
- [146] Ceriotti M, Cuny J, Parrinello M, et al. Nuclear quantum effects and hydrogen bond fluctuations in water. Proc Natl Acad Sci USA. 2013;110:15591-15596.
- [147] Li XZ, Walker B, Michaelides A. Quantum nature of the hydrogen bond. Proc Natl Acad Sci USA. 2011;108:6369-6373.
- [148] Nagata Y, Pool RE, Backus EHG, et al. Nuclear quantum effects affect bond orientation of water at the water-vapor interface. Phys Rev Lett. 2012;109:226101.
- Morrone JA, Car R. Nuclear quantum effects in water. Phys Rev Lett. 2008;101:017801.
- [150] Yang Z, Li YZ, Zhou GB, et al. Molecular dynamics simulations of hydrogen bond dynamics and far-infrared spectra of hydration water molecules around the mixed monolayer-protected au nanoparticle. J Phys Chem C. 2015;119:1768-1781.
- [151] Li YZ, Yang Z, Hu N, et al. Insights into hydrogen bond dynamics at the interface of the charged monolayer-protected au nanoparticle from molecular dynamics simulation. J Chem Phys. 2013;138:184703.
- Zhou GB, Yang Z, Fu FJ, et al. Molecular-level understanding of solvation structures and vibrational spectra of an ethylammonium nitrate ionic liquid around single-walled carbon nanotubes. Ind Eng Chem Res. 2015;54:8166-8174.
- [153] Zhou GB, Li YZ, Yang Z, et al. Structural properties and vibrational spectra of ethylammonium nitrate ionic liquid confined

- in single-walled carbon nanotubes. J Phys Chem C. 2016;120:5033-
- [154] Behler J. First principles neural network potentials for reactive simulations of large molecular and condensed systems. Angew Chem Int Edit. 2017;56:12828-12840.
- Quaranta V, Behler J, Hellstrom M. Structure and dynamics of the liquid-water/zinc-oxide interface from machine learning potential simulations. J Phys Chem C. 2019;123:1293-1304.
- [156] Behler J, Martonak R, Donadio D, et al. Metadynamics simulations of the high-pressure phases of silicon employing a highdimensional neural network potential. Phys Rev Lett. 2008;100:185501.
- [157] Boes JR, Kitchin JR. Modeling segregation on AuPd(111) surfaces with density functional theory and monte carlo simulations. J Phys Chem C. 2017;121:3479-3487.
- Artrith N, Kolpak AM. Grand canonical molecular dynamics simulations of Cu-Au nanoalloys in thermal equilibrium using reactive ann potentials. Comp Mater Sci. 2015;110:20-28.
- [159] Hellstrom M, Behler J. Structure of aqueous naoh solutions: insights from neural-network-based molecular dynamics simulations. Phys Chem Chem Phys. 2017;19:82-96.
- [160] Morawietz T, Singraber A, Dellago C, et al. How van der waals interactions determine the unique properties of water. Proc Natl Acad Sci USA. 2016;113:8368-8373.
- [161] Natarajan SK, Behler J. Neural network molecular dynamics simulations of solid-liquid interfaces: water at low-index copper surfaces. Phys Chem Chem Phys. 2016;18:28704-28725.
- [162] Quaranta V, Hellstrom M, Behler J. Proton-transfer mechanisms at the water-ZnO interface: The role of presolvation. J Phys Chem Lett. 2017;8:1476-1483.
- [163] Quaranta V, Hellstrom M, Behler J, et al. Maximally resolved anharmonic oh vibrational spectrum of the water/ZnO(1010) interface from a high-dimensional neural network potential. J Chem Phys. 2018;148:241720.
- Behler J. Perspective: machine learning potentials for atomistic simulations. J Chem Phys. 2016;145:170901.
- [165] Schmidt J, Marques MRG, Botti S, et al. Recent advances and applications of machine learning in solid-state materials science. NPJ Comput Mater. 2019;5:83.